Inorg. Chem. **2007**, *46*, 4951–4959

External Magnetic Field-Induced Mesoscopic Organization of Fe_3O_4 Pyramids and Carbon Sheets

S. V. Pol,[†] V. G. Pol,[†] A. Gedanken,*[,†] I. Felner,[‡] M-G Sung,[§] and S. Asai[§]

Department of Chemistry and Kanbar Laboratory for Nanomaterials at the Bar-Ilan University Center for Advanced Materials and Nanotechnology, Bar-Ilan University, Ramat-Gan 52900, Israel, Racah Institute of Physics, Hebrew University, Jerusalem 91904, Israel, and Department of Materials Processing Engineering, Graduate School of Engineering, Nagoya University, Furo-cho, Chikusa-ku, Nagoya 464-8603, Japan

Received January 22, 2007

The current investigation is centered on the thermal decomposition of iron(II) acetyl acetonate, $Fe(C_5H_7O_2)_2$, in a closed cell at 700 °C, which is conducted under a magnetic field (MF) of 10 T. The product is compared with a similar reaction that was carried out without a MF. This article shows how the reaction without a MF produces spherical Fe_3O_4 particles coated with carbon. The same reaction in the presence of a 10 T MF causes the rejection of the carbon from the surface of pyramid-shaped Fe_3O_4 particles, increases the Fe_3O_4 particle diameter, forms separate carbon particles, and leads to the formation of an anisotropic (long cigarlike) orientation of Fe_3O_4 pyramids and C sheets. The macroscopic orientation of Fe_3O_4 pyramids + C sheets is stable even after the removal of an external MF. The suggested process can be used to fabricate large arrays of uniform wires comprised of some magnetic nanoparticles, and to improve the magnetic properties of nanoscale magnetic materials. The probable mechanism is developed for the growth and assembly behavior of magnetic Fe_3O_4 pyramids + C sheets under an external MF. The effect of an applied MF to synthesize morphologically different, but structurally the same, products with mesoscopic organization is the key theme of the present paper.

Introduction

Mesoscopic structures of nanocrystals are becoming a rapidly growing field of science where the efforts of chemists, physicists, material scientists, and biologists are combined. A new field of research has recently emerged regarding the use of individual nanocrystals for growing 2D and 3D superstructures and investigation of the collective properties of these artificial quantum dot solids.[1] The fabrication of nanometer-order entities is considered to be the key for applications in data storage, functional devices, communications, and technology. The nanostructures, which are randomly distributed, fluctuate in size, have an unchanged periodicity, and possess significant limitations to their application. Thus, the ability to systematically manipulate these nanocrystals is an important goal in modern materials science.

Over the past decade, nanoscale magnetic materials have attracted intensive interest because of their potential application in high-density magnetic recording, in magnetic sensors, and in addressing some basic issues about magnetic phenomena in low-dimensional systems.[2,3] Various approaches have been developed to prepare nanoscale magnetic materials.[4−7] However, very little attention has been paid to the study of the effect of an external magnetic field (MF) on the nucleation and growth process of the magnetic materials and on the movement and self-assembly behavior of magnetic nanocrystallites. Indeed, it is found that a magnetic field can significantly influence the movement of magnetic particles. An interesting phenomenon is that migratory and

* To whom correspondence should be addressed. E-mail: gedanken@mail.biu.ac.il.
[†] Bar-Ilan University.
[‡] Hebrew University.
[§] Nagoya University.

(1) Pileni, M. P. *J. Phys. Chem. B* **2001**, *105*, 3358.
(2) Jun, Y.; Jung, Y.; Cheon, J. *J. Am.Chem. Soc.* **2002**, *124*, 615.
(3) Kim, B.; Tripp, S. L.; Wei, A. *J. Am. Chem. Soc.* **2001**, *123*, 7955.
(4) Srivastava, D. N.; Perkas, N.; Gedanken, A.; Felner, I. *J. Phys. Chem. B* **2002**, *106*, 1878.
(5) Wu, Y. H.; Qiao, P. W.; Qiu, J. J.; Chong, T.; Low, T. S. *Nano Lett.* **2002**, *2*, 161.
(6) Tripp, S. L.; Pusztay, S. V.; Ribbe, A. E.; Wei, A. *J. Am. Chem. Soc.* **2002**, *124*, 7914.
(7) Puntes, V. F.; Zanchet, D.; Erdonmez, C. K.; Alivisatos, A. P. *J. Am. Chem. Soc.* **2002**, *124*, 12874.

10.1021/ic070108g CCC: $37.00
Published on Web 05/08/2007

(a) (b) (c)

Figure 1. RAPET system: (a) the stainless steel Swagelok body filled with iron(II) acetyl acetonate under inert atmosphere, (b) the tubular furnace used for Swagelok heating, and (c) the homemade ceramic oven containing the Swagelok filled with 2 g of iron(II) acetyl acetonate, placed between the magnetic poles, applying a weak, 1 T MF.

homing animals, as well as bacteria, seem to possess a built-in compass which responds to the earth's magnetic field for navigation.[8−9] One hypothesis is that a dipolar-interaction-directed self-assembly process could give rise to chains. Mertl[10] suggests that iron-laden cells may provide these creatures with a legend to the earth's magnetic road map. These results imply that a MF would affect the growth and directional aggregation of nanocrystallites, resulting in the formation of self-assembly structures of magnetic materials. It is, therefore, significant to study the growth and assembly behavior of magnetic nanocrystallites under an external MF. The growth and assembly of cobalt nanocrystallites under an external MF of 0.25 T is known.[11] The external MF-induced growth of single crystalline Fe_3O_4 nanowires is reported by Wang et al. along the easy magnetic [111] or [110] axes.[12] Nanowires of $SrFe_{12}O_{19}$ with diameters of 100 nm and lengths of 2.5 mm have been successfully synthesized in a hydrothermal cell at 180 °C with an applied MF of 0.35 T.[13] Only arborescent aggregates are obtained in the electrochemical growth of iron under a MF of 0.6 T.[14] The surface morphology and growth mechanism of $YBa_2Cu_3O_7$ films by chemical vapor deposition in a MF of 2−8 T[15] are identified. Abu-Much et al. recently demonstrated the formation of a 3D microstructure of a Fe_3O_4−poly(vinyl alcohol) composite by evaporating the hydrosol under weak MF.[16]

In this article, a solvent-free, single-step, scalable, and straightforward approach is demonstrated for the anisotropic orientation of Fe_3O_4 pyramids + C sheets via implementing an external MF during their synthesis. The current research is centered on the thermal decomposition of iron(II) acetyl acetonate in a closed cell at 700 °C, which is performed under the application of a 10 T MF. The acquired products are compared with the analogous reaction that was carried out without a MF. This article illustrates how the reaction without a MF fabricates spherical Fe_3O_4 particles coated with carbon. In the presence of an applied 10 T MF, we observe the rejection of carbon from the surface of pyramid-shaped Fe_3O_4 particles, the increase in Fe_3O_4 particle diameter, formation of separate carbon sheets, and creates an anisotropic (long cigarlike) orientation of Fe_3O_4 pyramids + C sheets. The mesoscopic organization of solid Fe_3O_4 pyramids + C sheets is stable even after the removal of an external MF. The procedure can be used to fabricate large arrays of uniform wires comprised of some magnetic nanoparticles and improve the magnetic properties of nanoscale magnetic materials. Under the applied MF, a similar RAPET (reaction under autogenic pressure at elevated temperatures) route was implemented for the fabrication of MoO_2/carbon nanocomposites,[17] carbon filaments,[18] as well as for the rejection of ferromagnetic carbon from the surface of cobalt particles.[19]

Experimental Section

1. Fabrication of Fe_3O_4 Nanoparticles Coated with Carbon and Mesoscopic Organization of Pyramid-Shaped Fe_3O_4 Pyramids + C Sheets. Iron(II) acetyl acetonate [$Fe(C_5H_7O_2)_2$], was purchased from Aldrich with a purity >99% and was utilized without further purification. In the beginning, the fabrication of the Fe_3O_4 nanoparticles coated with carbon was obtained without applying a MF. Typically, 2 g of an iron(II) acetyl acetonate precursor was introduced into a 5 mL closed reactor assembled from stainless steel Swagelok parts (Figure 1a). For these syntheses, an iron(II) acetyl acetonate precursor was introduced into the reactor at room temperature (RT) under a nitrogen-filled glove box. The filled cell was closed tightly by the other cap and then placed inside an iron pipe in the middle of the furnace. The temperature was raised at a rate of 10 °C/min to 700 °C and maintained for 180 min at this temperature (Figure 1b). The chemical dissociation and transformation reaction took place under the autogenic pressure of the precursor. The Swagelok reactor was allowed to cool gradually (~250 min) to RT, opened, and a blackish powder was obtained.

(8) Walker, M. M.; Diebel, C. E.; Haugh, C. V.; Pankhurst, P. M.; Montgomery, J. C.; Green, C. R. *Nature* **1997**, *390*, 371.
(9) Hanzlik, M.; Winklhofer, M.; Petersen, N. *Earth Planetary Sci. Lett.* **1996**, *145*, 125.
(10) Mertl, M. *AAAS Meeting: Neurobiol. Sci.* **1999**, *283*, 775.
(11) Niu, H.; Chen, Q.; Zhu, H.; Lin, Y.; Zhang, X. *J. Mater. Chem.* **2003**, *13*, 1803.
(12) Wang, J.; Chen, Q.; Zheng, C.; Hou, B. *Adv. Mater.* **2004**, *16*, 137.
(13) Wang, J.; Zeng, C. *J. Cryst. Growth* **2004**, *270*, 729.
(14) Bodea, S.; Vignon, L.; Ballou, R.; Molho, P. *Phys. Rev. Lett.* **1999**, *83*, 2612.
(15) Ma, Y.; Watanabe, K.; Awaji, S.; Motokawa, M. *J. Cryst. Growth* **2001**, *233*, 483.
(16) Abu-Much, R.; Meridor, U.; Frydman, A.; Gedanken, A. *J. Phys. Chem B* **2006**, *110*, 8194.
(17) Pol, S. V.; Pol, V. G.; Kessler, V. G.; Seisenbaeva, G. A.; Sung, M.; Asai, S.; Gedanken, A. *J. Phys. Chem B* **2004**, *108*, 6322.
(18) Pol, V. G.; Pol, S. V.; Gedanken, A.; Sung, M.; Asai, S. *Carbon* **2004**, *13*, 2738.
(19) Pol, V. G.; Pol, S.V.; Gedanken, A.; Kessler, V. G.; Seisenbaeva, G. A.; Sung, M.-G.; Asai, S. *J. Phys. Chem. B* **2005**, *109*, 6121.

The total yield of the product/carbonaceous materials was about 48.4% of the iron(II) acetyl acetonate precursor. The yield is the final weight of the product relative to the weight of the starting material. The obtained material is termed a "carbon coated iron oxide" (CCIO) sample.

In the second reaction, the identical procedure was carried out under a static MF of 10 T, which was generated using a helium-free superconducting magnet. The analogous control reaction was also carried out employing a low (1 T) MF to check the efficacy of the applied MF. The Swagelok containing the iron(II) acetyl acetonate precursor was set in the maximum magnetic point in the bore of the magnet, where the gradient of the MF was the smallest. A ceramic oven containing the Swagelok filled with 2 g of iron(II) acetyl acetonate was positioned between the magnetic poles (Figure 1c). The oven was heated and cooled at the same heating and cooling rates as those for a reaction without a MF. The yield of the product was around 47%. This is termed an "iron oxide−carbon composite prepared under a magnetic field" (IOCMF) sample. Approximately the same yields are achieved in the reaction carried out without and with the magnetic fields (1 or 10 T).

2. Instrumental. XRD patterns were collected by a Bruker AXS D* Advance Powder X-ray Diffractometer (Cu Kα radiation, wavelength 1.5406 Å). The morphologies and nanostructure of the as-synthesized products were further characterized by JEM-1200EX, TEM, and JEOL-2010 HRTEM instruments, with accelerating voltages of 80 and 200 kV, respectively. The elemental compositions of the materials were analyzed by an energy-dispersive X-ray analysis technique connected to a scanning electron microscope (HR-SEM, JSM, 7000 F). The same instrument was used to acquire the SEM images of CCIO and IOCMF products and the 1D assembly of IOCMF without a gold coating. Samples for TEM and HRTEM were prepared by ultrasonically dispersing the products into absolute ethanol, placing a drop of this suspension onto a copper grid coated with an amorphous carbon film, and then drying under air. Mössbauer spectroscopy (MS) studies were carried out at RT using a conventional constant-acceleration spectrometer. The ^{57}Fe MS were measured with a 50 mCi ^{57}Co: the Rh source and the spectra were least-square fitted with two subspectra. The isomer shift (IS) values are relative to Fe metal at 300 K. Specific surface areas were measured by the Brunaur−Emmett−Teller (BET) method at 77 K using N_2 gas as an absorbent after heating the sample at 120 °C for 1 h. The elemental analysis of the samples was carried out by an Eager 200 C, H, N, S analyzer. An Olympus BX41 (Jobin−Yvon−Horiba) Raman spectrometer was employed, using the 632.8 nm line of an He−Ne laser as the excitation source focused on a 1−2 μm spot size to analyze the nature of the carbon present in CCIO and IOCMF products. TGA (TGA Q 500) coupled with a mass spectrometer [PFEIFFER Vacuum] was used to study the thermal decomposition process of iron(II) acetyl acetonate under inert atmosphere.

Results and Discussion

The major visible and noticeable differences between the sample prepared without MF (CCIO) and with MF (IOCMF) are as follows. The CCIO sample is dark black and in powder form, while the IOCMF sample is grayish and in the form of long cigarlike dry flakes. The observed flakes are as long as the Swagelok length (∼3 in.), and after opening the Swagelok reactor, the flakes dispersed and separated. An optical microscope was used for imaging the long cigarlike shapes at the lowest magnification (see Figure 2a). The measured length was 1 cm, with a diameter of several micrometers. The physical impact or handling of the samples with a pin set or a spatula breaks these cigarlike flakes into a 1D entity. The morphological difference between the CCIO and IOCMF samples was further verified by HR-SEM analysis. Figure 2b demonstrates the morphology of the CCIO sample. Big agglomerates having a diameter of more than a micrometer were observed. The picture shows spheres, as well as rods and unshaped particles, as the products. On the other hand, in the IOCMF sample, a 1D entity, 10−200 μm long with a diameter of several micrometers (Figure 2c) is observed as the products under a MF of 10 T. The smallest broken part of the IOCMF sample also showed a 1D arrangement of the comprised particles. The HR-SEM image (Figure 2d) illustrates that the small 1 μm diameter aggregates of pyramid-shaped particles are chained together and form several chains aligned parallel to each other. These chains are comprised of Fe_3O_4 particles and carbon bodies, confirmed by the EDS analysis presented in Figure 2e. The morphological and structural details of CCIO and IOPMF samples are observed and studied, employing TEM and HR-TEM measurements.

The transmission electron micrograph of the CCIO sample is shown in Figure 3a. It depicts dark spherical nanoparticles surrounded by a faint material forming a core−shell structure in the absence of a MF. These dark nanoparticles are identified as the Fe_3O_4 core homogeneously embedded in a carbon shell. The assignment of the core to Fe_3O_4 and the shell as carbon is based on measured SAEDS (Figure 3b). The strong carbon signal results of a 35 nm electron beam focused on the outer shell of the Fe_3O_4 particle showing a high amount of carbon, originated from the carbon shell. The core of the sample is a Fe_3O_4 particle, evidenced when a 35 nm electron beam is focused on a single Fe_3O_4 particle from the CCIO sample. An intense peak assigned to Fe_3O_4 and a weak carbon peak, are detected (insert of Figure 3b). The Cu peaks originated from the TEM grid. Thus, the SAEDS results further provide the compositional information of the CCIO sample. Due to the surrounding carbon shell, the Fe_3O_4 core particles are not agglomerated. The diameter of these Fe_3O_4 nanoparticles ranges between 15 and 50 nm. The high-resolution TEM image (Figure 3c) reveals a 15 nm Fe_3O_4 crystalline core, surrounded by an ∼10 nm carbon shell. On the other hand, in the IOCMF product the TEM picture illustrates trigonal or pyramid-shaped particles, which *are not* coated with a nanolayer of carbon (Figure 3d). This particular picture, Figure 3d, is focused on the Fe_3O_4 particles, while Figure 3e focuses on the carbon bodies. The carbon produced under a MF is random in shape and size. The formed carbon during the thermal decomposition of iron-(II) acetyl acetonate is mostly disordered, owing to an insufficient temperature (700 °C) for forming graphitic ordering. The nature of formed carbon with and without MF is determined by Raman spectroscopy and is presented in the following section. Another peculiarity is that the particles fabricated under a MF are bigger than those synthesized without a MF. The diameter of the obtained Fe_3O_4 particles under a MF varies between 200 and 1000 nm. We could not find on the TEM grid a carbon-coated Fe_3O_4 particle resulting

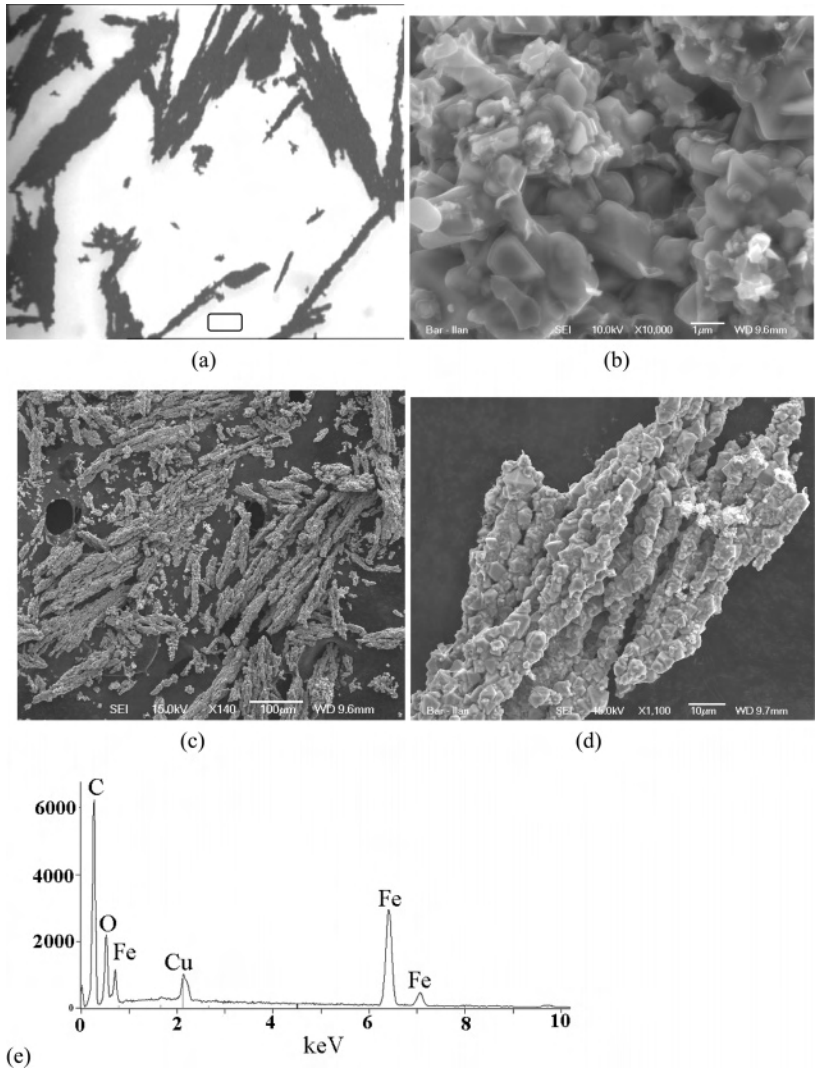

Figure 2. (a) Optical microscope image of an IOCMF sample showing long cigarlike flakes (scale bar = 1 mm). (b) The SEM image of a CCIO sample. (c) The SEM image of an IOCMF sample. (d) The high-resolution SEM image of an IOCMF sample. (e) The EDS of an IOCMF sample.

from a RAPET reaction in a MF. The acquired larger particles under the influence of the MF can be explained as the result of the lack of carbon coating, which allows theFe_3O_4 particles to grow freely. The electron diffraction (ED) pattern taken on the pyramid-shaped Fe_3O_4 particle is depicted in Figure 3f. The acquired diffraction reflects a typical hexagonal pattern. The HR-TEM (Figure 3g) provides further evidence for the identification of the product as Fe_3O_4, illustrating the ideal arrangement of the atomic layers. The measured distance between these (220) lattice planes is 0.297 nm, which is very close to the distance between the planes reported in the literature (0.2968 nm) for the face-centered cubic lattice of the Fe_3O_4 (PDF No. 65-3107).

Elemental analysis was employed to determine the carbon, oxygen, and hydrogen content in the product/carbonaceous materials. The calculated element (wt) percent in the reactants matched that of the obtained elemental analysis data for the products. The calculated element percent of C, H, O, and Fe in $Fe(C_5H_7O_2)_2$ was 47.28%, 5.51%, 25.21%, and 22%, respectively. The measured element percentage of carbon in the IOCC product was 36.46%, hydrogen 0.4%, while oxygen was 17.56%. The calculated weight of metal Fe was 440 mg in 2 g of iron(II) acetyl acetonate precursor, while 445 mg accounted for the 968 mg of the CCIO product. The sample prepared in a MF (IOPMF) shows 34.87% carbon, 0.5% hydrogen, and 18% oxygen, while 443 mg of metal Fe is accounted for in the 940 mg of the IOCMF product. It is suggested that the weight loss of carbon, oxygen, and hydrogen is due to the formation of hydrocarbons[20] and CO_2 that exist in the cell as a result of the high pressure. On the other hand, no loss of iron was observed as expected, since no volatile compounds of iron were formed.

Raman spectroscopy measurements were performed in order to understand the nature of the carbon in these samples. The micro-Raman spectra of CCIO (i) and IOPMF (ii) samples are shown in Figure 4, in which a broad peak at 1334 cm^{-1}, as well as a comparatively sharp absorption peak at 1596 cm^{-1}, can be clearly seen. The peak at 1334 cm^{-1} is usually associated with the vibrations of carbon atoms with dangling bonds for the in-plane terminations of disordered graphite, and is labeled as the D-band. The peak at 1590 cm^{-1} (G-band) (corresponding to the E_{2g} mode) is closely

(20) Pol, S. V.; Pol, V. G.; Gedanken, A. *Chem. Eur. J.* **2004**, *10*, 4467.

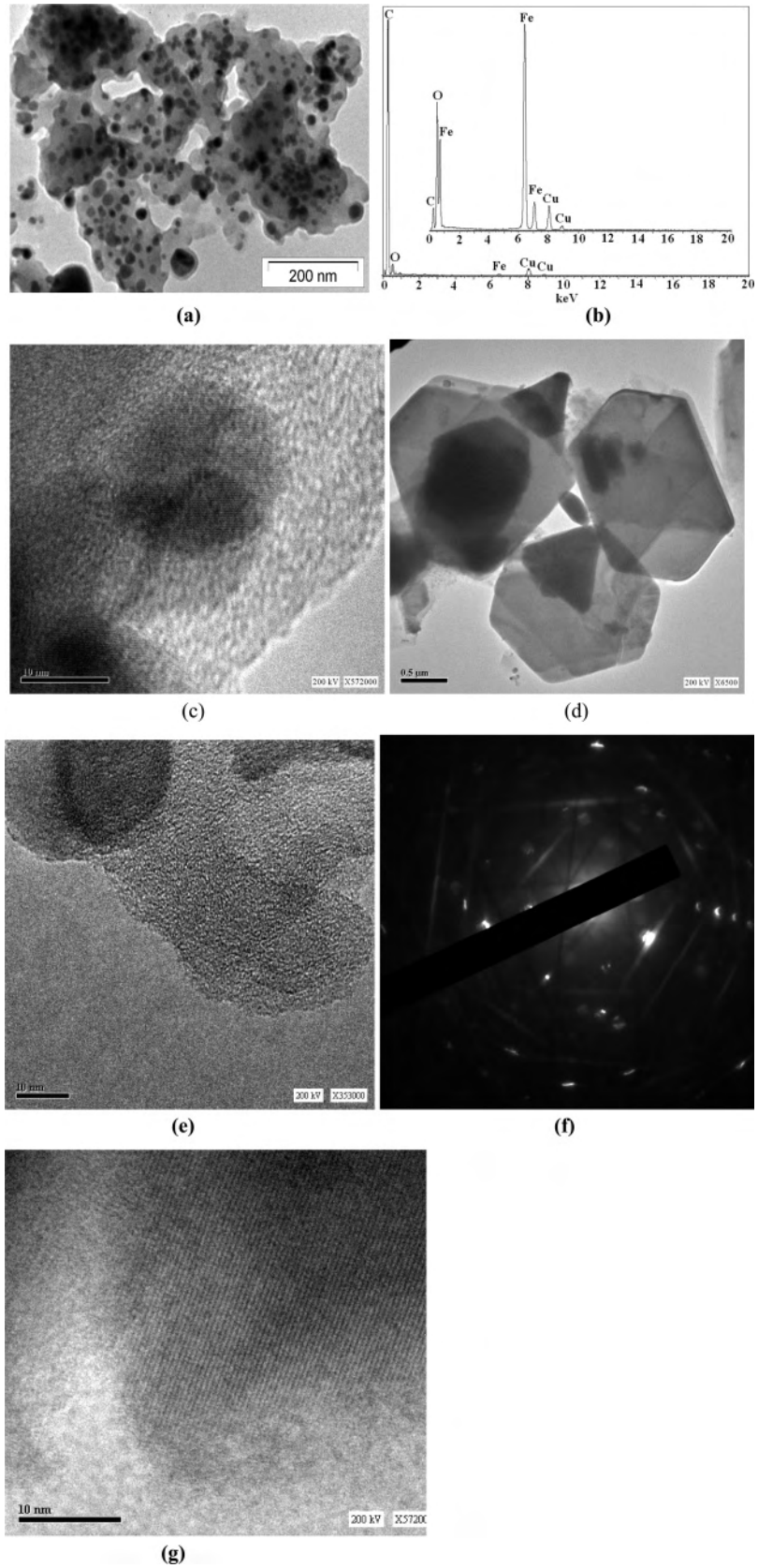

Figure 3. Transmission electron micrographs of (a) the CCIO sample (b) the selected area energy dispersive X-ray analysis of the CCIO sample focused on carbon. The insert focuses on a Fe_3O_4 particle. (c) HR-TEM of the CCIO sample. (d) The IOCMF demonstrates the pyramid shape of Fe_3O_4 formed under the application of a MF. (e) The rejected carbon from the Fe_3O_4 core due to an applied MF. (f) The obtained electron diffraction pattern for a Fe_3O_4 particle. (g) Interlayer spacing of a Fe_3O_4 particle.

related to the vibration in all sp^2-bonded carbon atoms in a 2D hexagonal lattice, such as in a graphene layer.[20,21] The intensity ratio of the D to G band (I_D/I_G) is calculated as 0.96 and 1.03 for the CCIO and IOCMF samples, respec-

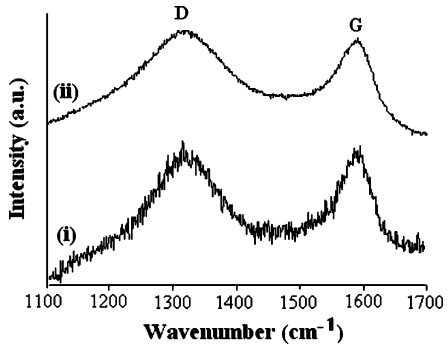

Figure 4. Raman spectra of CCIO (i) and IOPMF (ii) samples.

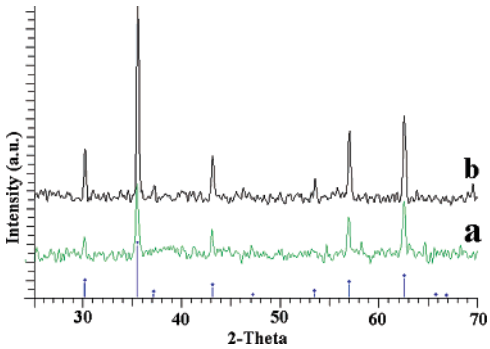

Figure 5. X-ray patterns of (a) a CCIO sample and (b) an IOCMF sample.

tively, further reflecting the relative formation of disordered and graphitic carbon.

The measured surface areas for the CCIO and IOCMF products are 1.27 and 2.25 m^2/g, respectively. The obtained surface areas for CCIO product are the result of the smaller size Fe_3O_4 particles coated by carbon.

The crystalline structure and purity measurements of the as-synthesized CCIO (a) and IOCMF (b) samples were examined by powder XRD (Figure 5). The major diffraction peaks were observed at $2\theta = 30.10$, 35.45, 37.08, 43.08, 53.45, 56.98, 62.57, and 74.02 and were assigned as (220), (311), (222), (400), (422), (511), (440), and (533) reflection lines. These values are in good agreement with the diffraction peaks, peak intensities, and cell parameters of crystalline Fe_3O_4 (PDF No. 65-3107). The XRD peaks for the IOCMF are more intense than those of the CCIO sample, owing to the absence of carbon on the Fe_3O_4 particles' surface. As anticipated, the peak broadening corresponds to the smaller diameter of Fe_3O_4 particle is not observed for the CCIO sample.

However, since the XRD of γ-Fe_2O_3 is very similar to that of magnetite, we also used Mössbauer spectroscopy to further substantiate our assignment. Similar Mössbauer spectra were obtained for the CCIO and IOCMF samples. The representative Mössbauer spectrum of IOCMF sample at 298 K is shown in Figure 6. The spectrum shows two hyperfine magnetic splittings, which is clear evidence for the existence of Fe_3O_4 (magnetite). The resultant parameters are given in Table 1. Fe_3O_4 can be written as $[(Fe^{3+})(Fe^{2+}\text{-}Fe^{3+})]O_4$. The magnetic hyperfine fields of 455 and 487 kOe

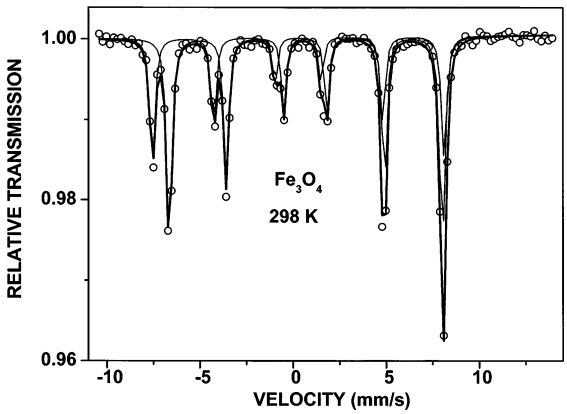

Figure 6. Mössbauer spectrum of an IOCMF sample at room temperature.

Table 1. Mössbauer Parameters of the IOCMF Sample: Isomeric Shift (mm/s), Quadrupole Moment (mm/s) and Effective Field (kOe) for Sites A and B

	IS (mm/s)	1/2eq$Q$ (mm/s)	H_{eff} (kOe)
site A	0.67	0.028	455
site B	0.37	−	487

and the two isomer shift values 0.67 and 0.37 mm/s correspond to site A (Fe^{3+}) ions and to site B (Fe^{2+}, Fe^{3+}) ions,[23] respectively. The high isomer shift for the B site is typical for Fe^{2+}.

A RT magnetic susceptibility measurement of CCIO and IOCMF samples was conducted by employing a vibrating sample magnetometer (VSM). A small amount of material, ~30 mg, was inserted into a gelatin capsule. Cotton wool was placed on top of the sample, and the capsule was sealed. This prevents the particles from any movement caused by the vibration of the VSM sample holder rod or by a variation of the applied magnetic field during the measurements.

The CCIO sample illustrates the maximum magnetization of 31 emu/g (Figure 7a). Taking into account that the sample contains 63.53% of Fe_3O_4 particles, this gives a value of 48.8 emu/g, assuming 100% Fe_3O_4 particles. The IOCMF sample exhibits typical hysteresis with a saturation magnetization of 40 emu/g (Figure 7b). Considering that the IOCMF sample contains 34.87% carbon, the remaining 65.13% of Fe_3O_4 yields a value of 61.41 emu/g for 100% Fe_3O_4. Note that the IOCMF sample, the coercive field, is 110 Oe, and the remanent magnetization is 7emu/g. Therefore, we ensure that this compound is ferromagnetically ordered. On the other hand, for CCIO, the characteristic behavior of superparamagnetism is observed. This superparamagnetic nature is demonstrated in the magnetization curve, which does not show hysteresis. It does not saturate, even at 16 kOe for the CCIO sample, and is due to the small size, 15 nm, Fe_3O_4 crystalline core (shown in TEM measurements). The magnetization of ferromagnetic materials is very sensitive to the microstructure of a sample. If a specimen consists of small particles, its total magnetization decreases

(21) Hu, G.; Cheng, M. J.; Ma, D.; Bao, X. H. *Chem. Mater.* **2003**, *15*, 1470.

(22) Dresselhaus, M. S.; Dresselhaus, G.; Pimenta, M. A.; Eklund, P. C. In *Analytical Applications of Raman Spectroscopy*; Pelletier, M. J., Ed.; Blackwell Science: Oxford, 1999; Chapter 9.

(23) Vijayakumar, R.; Koltypin, Y.; Felner, I.; Gedanken, A. *Mater. Sci. Eng. A* **2000**, *286*, 101.

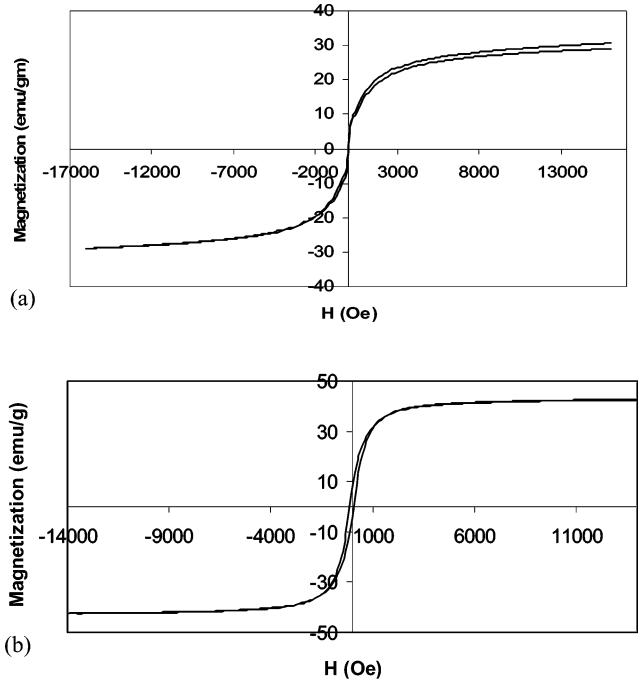

Figure 7. Magnetization vs magnetic field curves for (a) CCIO and (b) IOCMF samples measured at room temperature.

with the decreasing particle size due to the increased dispersion in the exchange integral,[25] and finally, reaches the superparamagnetic state, when each particle acts as a big 'spin' with suppressed exchange interaction between the particles, which is more hindered because of the presence of a carbon shell. Nanomagnetic particles are expected to exhibit reduced magnetization due to the large percentage of surface spins with disordered magnetization orientation.[26] In fact, the magnetization is smaller than the bare particles, indicating that there is no magnetic proximity effect between the magnetic Fe_3O_4 particles and carbon. This is consistent with recent experiments.[27] The microwave-synthesized pure Fe_3O_4 nanoparticles (8−9 nm) depict the M_s of ∼65 emu/g.[24] Our obtained M_s values for pure Fe_3O_4 are closer for the IOCMF sample, while a smaller value is measured for the CCIO sample, which is probably because of the coated carbon.

Still, there are a few open questions that have yet to be answered.

(1) Why are Fe_3O_4 particles coated with carbon when the decomposition reaction is carried out without MF, while the carbon particles are separated from Fe_3O_4 particles when 10 T MF is applied?

(2) Why are spherical Fe_3O_4 particles obtained without MF, while pyramid-shaped particles are formed under MF?

(3) Why is a mesoscopic organization of Fe_3O_4 pyramids + C sheets dominant under the applied MF?

To learn about the decomposition products of iron(II) acetyl acetonate,TGA coupled with mass spectroscopy analysis was carried out up to 700 °C under inert atmosphere. The results are presented in Figure 8. The total weight losses are observed in three steps. The green curve indicates percent weight loss with respect to temperature, while the blue curve represents its derivative. The major (∼66%) weight loss is observed below 300 °C, minor (4%) at 350 °C, and an additional 7.7% is detected at 645 °C. The major decomposition of the iron(II) acetyl acetonate might have occurred below 600 °C. However, below 600 °C, we did not receive any crystalline products. That is the reason why the RAPET reactions are conducted at 700 °C. In the case of Fe acetyl acetonate, the reactant possesses a +2 oxidation state, while the product has an oxidation state of 2.66. This means that part of the original Fe^{+2} is oxidized. In both cases of CCIO and IOCMF, partially oxidized products are detected, confirming that there is no influence of coated carbon on the surface of the iron oxides. This indicates that the formation of Fe_3O_4 occurs prior to that of carbon coating. The TGA recorded a total weight loss of 77.7% below 700 °C under a flow of nitrogen, leaving a 22.3% product. These 22.3% weights are identical to the iron content in the precursor formula that remains in the TGA pan. On dissociation of the Iron(II) acetyl acetonate, C_2H_2 (m/e = 25), C_3H_6 (42), CO_2 (44), C (12), and acetone, CH_3COCH_3 (58), escape, mostly below 300 °C, as confirmed by mass spectroscopy. Once again, 4% at 350 °C and 7.7% at ∼650 °C weight losses are observed in the mass spectrum as C (m/e = 12). The detected m/e = 12 might have originated from the dissociation of hydrocarbons under electron bombardment inside the mass spectrometer (MS), and not from the gaseous carbon. While the dissociation of iron(II) acetyl acetonate in a closed RAPET system at 700 °C confirmed the weight loss of 53%, keeping ∼47% of a solid product consisting of Fe_3O_4 (29.86%) and carbon (17.16%). The rest of the weight loss is due to the formation of hydrocarbons and carbon oxides.

The products of the dissociation reaction float in the gas phase and solidify right after their formation. The question is what solidifies first and what determines the order of solidification. In the case of the RAPET reaction of tetraethylorthosilicate (TEOS), we could account for the solidification of the carbon[28] as the spherical core, both thermodynamically and kinetically, and as being the more stable product. While in case of the RAPET reaction of $Mo(OMe)_4$, the formation[17] of a MoO_2 core coated with a carbon shell is explained on the basis of kinetics. In the dissociation of iron(II) acetyl acetonate, iron is already formed at 300 °C. Other dissociation products are hydrocarbons, carbon, hydrogen, and oxygen. Upon further heating, Fe_3O_4 is formed. The ordering of the crystallization in the present reaction can be explained only on a kinetics basis. Since the boiling and melting points of carbon are much higher than those of the transition metal oxides, thermodynamic carbon would,

(24) Hong, R. Y.; Pan, T. T.; Li, H. Z. *J. Magn. Magn. Mater.* **2006**, *303*, 60.
(25) Elliott, S. R. *Physics of Amorphous Materials*; Longman: London, New York, 1984; p 350.
(26) Kodoma, H. R.; Berkovitz, A. E.; Mcniff, E. J., Jr.; Foner, S. *Phys. Rev. Lett.* **1996**, *77*, 394.
(27) Hohne, R.; Ziese, M.; Esquinazi, P. *Carbon* **2004**, *42*, 3109.
(28) (a) Pol, V. G.; Pol, S. V.; Gedanken, A.; Goffer, Y. *J. Mater. Chem.* **2004**, *14*, 966. (b) Ayache, J.; Oberlin, A.; Inagaki, M. *Carbon* **1990**, *28*, 353. (c) Inagaki, M. *Carbon* **1997**, *35*, 711.

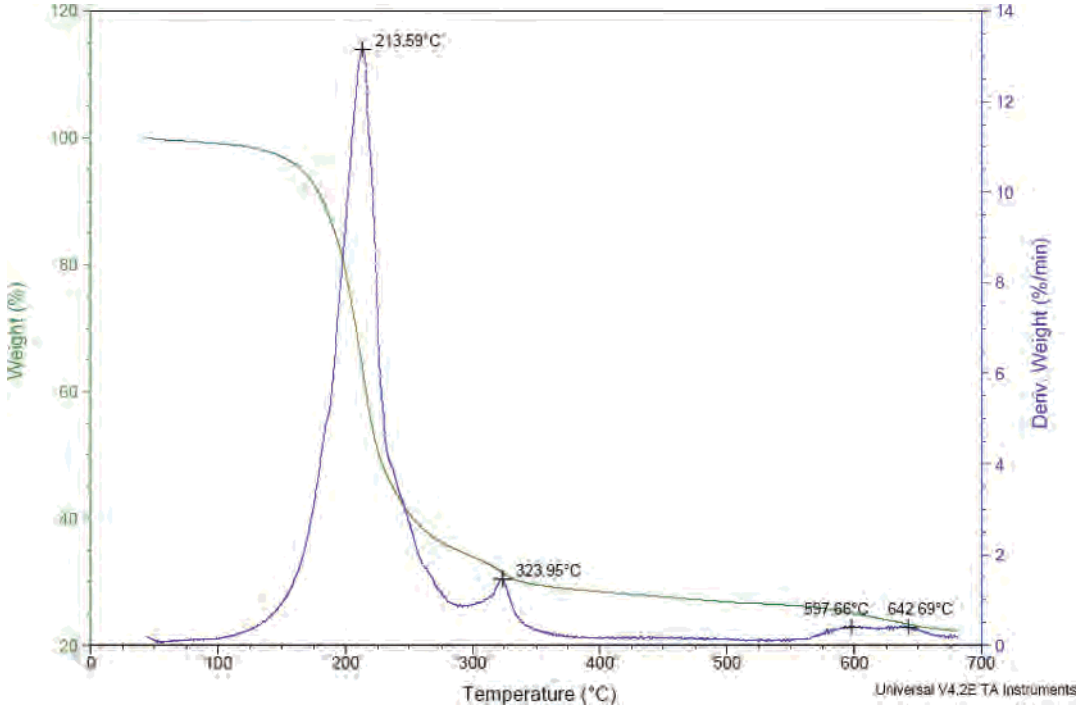

Figure 8. TGA curve of iron(II) acetyl acetonate carried out under inert atmosphere.

therefore, tend more easily to become a solid at 700 °C. In other words, from the thermodynamic point of view, carbon would be the first to solidify and form the core, and the Fe_3O_4 would create the shell if the two products were formed at the same temperature. However, since the process is kinetically controlled, the opposite occurs. Namely, Fe_3O_4 has a much higher solidification rate than carbon for forming the core of the composite. Another possibility is that the order is dictated by thermodynamics, namely, Fe_3O_4 is formed at a lower temperature than the dissociation of the hydrocarbons, to form carbon. Carbon is composed of an aromatic substance, i.e., basic surface units (BSUs). It is reported[28b,c] that when there are some solid impurities present, the carbon layers tend to align by arranging their basal planes parallel to the surface of the solid. Thus, carbon having a slower solidification rate forms the shell layer on the Fe_3O_4 core and becomes stable. In the present system, this is true when the reaction is carried out without a magnetic field.

Under an applied 10 T MF, the magnetic rejection of carbon from the surface of Fe_3O_4, forming separated carbon sheets, increases in particle size and the formation of an anisotropic (long cigarlike) orientated Fe_3O_4 pyramids is noted. Ferromagnetic Fe, Ni, and Co are well known as catalysts for the growth of carbon around it.[29] In the present system, in the absence of a MF, a carbon shell is formed around the Fe_3O_4 particles. Carbon nanotube synthesis using magnetic fluids (Fe_3O_4 nanoparticles) on various substrates is also reported.[30] In the magnetic field, the Fe_3O_4 particle becomes a permanent magnet, and thus, a magnetic line would be formed in the direction perpendicular to the surface of the Fe_3O_4 particle and an aromatic substance would align along the magnetic line. Such a stable arrangement would eventually lead to carbon sheets separated from the Fe_3O_4 particle. The rejection of carbon occurs due to magnetic forces between the magnetic Fe_3O_4 particles and the approaching carbon particles. The carbon surface is also known to be paramagnetic,[31] as demonstrated by ESR measurements. Whether ferromagnetic carbon exists[32] or not is not clear. However, the structure of the ferromagnetic carbon (equal number of sp^2- and sp^3-hybridized carbon atoms) is suggested by Ovchinnikov et al. and Shamovsky.[33] The carbon formed upon this dissociation has a strong interaction with the magnetic Fe_3O_4 particles, leading to its rejection from the surface of the substrate. Upon cooling, the IOCMF product fabricated in a MF at 700 °C/3 h causes the formation of Fe_3O_4 particles, which solidify first and reject any approaching magnetic carbon moiety. Similar carbon rejection processes occurred from the ferromagnetic Co[19] and the paramagnetic MoO_2 surfaces.[17]

Our scanning electron microscopy and transmission electron microscopy confirmed that spherical Fe_3O_4 particles are obtained without MF, while in applied MF (IOCMF products) perfect single Fe_3O_4 crystals with pyramidlike shapes are formed. Magnetite (Fe_3O_4) is a natural magnet.

Fe_3O_4 coated with a carbon nanocomposite formed without a 10 T MF have no clear alignment (Figure 2b), but the products created under a 10 T external MF have linear chains consisting of Fe_3O_4 pyramids (Figure 2a, c, and d). Figure

(29) Flahaut, E.; Govindaraj, A.; Peigney, A.; Laurent, C.; Rousset, A.; Rao, C. N. R. *1 Source: Chem. Phy. Lett.* **1999**, *300*, 236.
(30) Cho, Y. S.; Choi, G. S.; Kim, D. J.; Kim, H. J.; Yoon, S. G. *Met. Mater. Int*. **2003**, *9*, 427.
(31) Mrozowski, S. *Carbon* **1988**, *26*, 521.
(32) Makarova, T. L.; Sundqvist, B.; Hohne, R.; Esquinazi, P.; Kopelevich, Y.; Scharff, P.; Davydov, V. A.; Kashevarova, L. S.; Rakhmanina, A. V. *Nature* **2001**, *413*, 716.
(33) Ovchinnikov, A. A.; Shamovsky, I. L. *Theochems-J. Mol. Struct*. **1991**, *83*, 133.

2b also shows interlinks between spherical particles in arbitrary directions for the sample formed without an external MF. Ferromagnetic pyramid-shaped Fe_3O_4 particles magnetize one another by dipolar interaction in arbitrary directions. In the perfect single Fe_3O_4 crystals, the orientation of each domain is spontaneously random when no external MF is applied. However, when an external MF is applied, the pyramidal particles tend to align along the magnetic line of force and favor the formation of linear chains. Magnetization makes all single-domain particles orientate along the magnetic line of force. As a result, dipole-directed self-assembly through dipolar interaction[11] along the magnetic line of force could happen, leading to the formation of linear chains. The magnetic moment, magnetic field, and magnetic interactions on Fe_3O_4 crystals increase due to an applied MF. Under the attraction of an external MF, cigarlike entities are formed through pyramidal particle connections (Figure 2d) and the paramagnetic carbon diffuses to form separated sheets. The cigarlike chains are nearly parallel, which could be the result of magnetic attraction, resulting in the chains aligning parallel to the magnetic line of force.

An additional control reaction is carried out by applying a 1 T external MF. This reaction leads to the formation of mostly Fe_3O_4 particles coated with carbon. At this low magnetic field, only ~10% of the Fe_3O_4 particles are observed with a complete or partially removed carbon shell. Ninety percent of the magnetite nanoparticles are surrounded by the carbon shell, thus demonstrating the importance of the high magnetic field. The results suggest that a magnetic field greater than 1 T is required for the complete rejection of carbon off the surface of Fe_3O_4 particles.

Conclusions

The results of the thermal decomposition of iron(II) acetyl acetonate in a closed reactor at 700 °C conducted under the application of a 10 T MF are presented, and the obtained product is compared with a similar reaction carried out without a MF. The reaction without a MF produces spherical Fe_3O_4 particles coated with carbon, while in the presence of an applied 10 T MF, the rejection of carbon coating from the surface yields pyramid-shaped Fe_3O_4 particles. In addition, the formation of stable anisotropic (long cigarlike) Fe_3O_4 pyramids + C sheets are acquired under an external MF. The probable mechanism is developed and described for the growth and assembly behavior of magnetic Fe_3O_4 pyramids + C sheets under an external MF.

Acknowledgment. A. Gedanken thanks the Israeli Ministry of Science, Culture snd Sport for supporting this research through the strategic-generic program.

IC070108G